



24th COBEM - 2017



24th ABCM International Congress of Mechanical Engineering
December 3-8, 2017, Curitiba, PR, Brazil

COBEM-2017- 1945

THE FREEZE CASTING METHOD AS A PRODUCTION ALTERNATIVE FOR CERAMIC CAPILLARY EVAPORATORS

Frederico Marques Baumgratz ¹

Marcos Vinicio Oro ¹

Marcio Celso Fredel ²

Edson Bazzo ¹

Federal University of Santa Catarina, Department of Mechanical Engineering

¹LabCET - Laboratory of Combustion and Thermal Systems Engineering

²CERMAT - Ceramic & Composite Materials Research Laboratories

Campus Universitário, 88.040-900, Florianópolis, SC, Brazil

fredbaumgratz@gmail.com; oro@labcet.ufsc.br; e.bazzo@ufsc.br.

Abstract. An alternative method for the production of ceramic wicks for a capillary pumped loop (CPL) is presented. The freeze casting method is considered to provide a desired distribution of the size porous along the wick structure in order to maximize the capillary pressure required for CPL systems. The characterization of the structure is also presented, including porosity, critical diameter, capillary pressure and permeability. Two different slurries were prepared varying the water/solid ratio, wherein group A corresponds to 50 wt% alumina and 50 wt% water and group B, 65 wt% alumina and 35 wt% water. For both, groups A and B, an average porosity of about 57.1 and 64.7 %, critical diameters of 10.91 and 21.81 μm , a permeability of 5.45×10^{-13} and $1.95 \times 10^{-13} \text{ m}^2$ and capillary pumping pressure of 26.4 and 13.2 kPa were found, respectively. The measured characteristics meet the reference characteristics found in technical literature as well in successfully tested evaporators.

Keywords: CPL, Capillary pumped loop, Freeze casting, Alumina, Ceramic wick.

1. INTRODUCTION

The continuous development of electronic technologies brings with a crucial problem relate to thermal management of this components. In general, heat pipes have been used as heat transfer devices, but a serious constraint on conventional heat pipes is the reduction of transport capabilities when the condenser section is located very far or even below the evaporator section, especially in case of ground application. Therefore, it is logical to develop heat transfer devices capable of operating effectively at any orientation in a gravitational field over long distances. Capillary pumped loops (CPL) and loop heat pipes (LHP) are promise devices to solve such problems. A CPL is a reliable and versatile two phase heat transfer systems for applications requiring large heat loads over long distances (see Faghri, 1995). As shown in Figure 1, it operates in the following way: the heat applied onto the evaporator causes the evaporation of a selected working fluid (ammonia, acetone, water etc), so that the vapor flows to the condenser section through the vapor transport lines. At this point heat is removed and the vapor is condensed back to the liquid phase. Here, in order to eliminate any remaining vapor bubbles, the condenser section is designed to further reduce the temperature of the liquid below the saturation temperature. Finally, the liquid flows back to the evaporator by capillary action to complete the loop. A reservoir is used for startups and to stabilize the system, controlling the operating temperature. The wick structure is located in the evaporator section.

The CPL makes use of capillary forces provided by porous wick materials, to pump the working fluid through the system. However, also the wick structures are responsible for the pressure drop along the capillary evaporator. The small the pore sizes the higher the capillary pumping pressure but also the higher the fluid pressure drop through the evaporator.

Most CPLs use polyethylene or metallic porous wicks in the evaporator (Chen and Lin, 2001; Reimbrecht et al., 1999). Only few CPLs use ceramic porous wick. First works have been developed considering mulita and alumina as raw material (Berti et al., 2011; Reimbrecht et al., 2001).

The main objective of this work is to show a new fabrication method of ceramic wicks evaporator, with the required properties, as pore sizes, porosity and permeability. The proposed method is the freeze casting.

According to Lu, Qu, Zhou (1998) and Sofie, Dogan (2001) *apud* S. Deville (Deville, 2008), freeze casting has been first developed as a near net shape forming technique, yielding dense ceramics parts with fine replicate of the mold details. Any ice crystal being converted into porosity later in the process, introducing large size defects largely unwelcome in ceramic applications, a great deal of efforts has been put in controlling or avoiding the formation of ice crystals. Only later on, it was realized that the formation and growth of ice crystals could be a substantial benefit if properly controlled, yielding porous ceramics with a very specific porosity (Deschamps, 2016; Zhang et al., 2010).

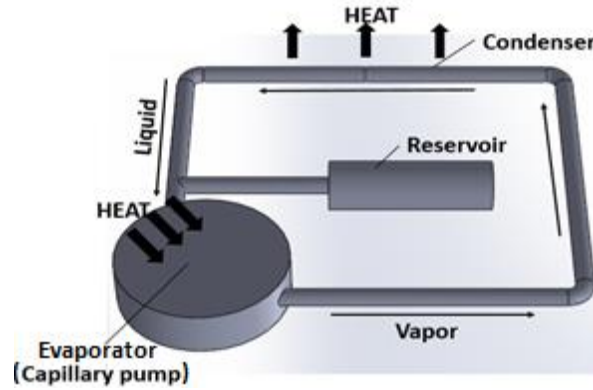


Figure 1. Schematic view of a CPL

2. EXPERIMENTAL PROCEDURE

The freeze casting method gives, for a fixed composition, different pore sizes that are controlled by the freezing rate. During the freezing process, the particles are expelled from the moving solidification front, and pile up between the vehicle crystals until the process completed. Subsequently, sublimation of the vehicle is done to eliminate the drying stresses, avoiding shrinkage, cracks and warping of the green parts that generally existing in the normal drying. Finally, the porous materials with a lamellar or/and columnar continuous microstructure are obtained by sintering (Wegst et al., 2010; Zhang et al., 2010). A schematic overview of the process, using the water phase diagram, is illustrated in Figure 2.

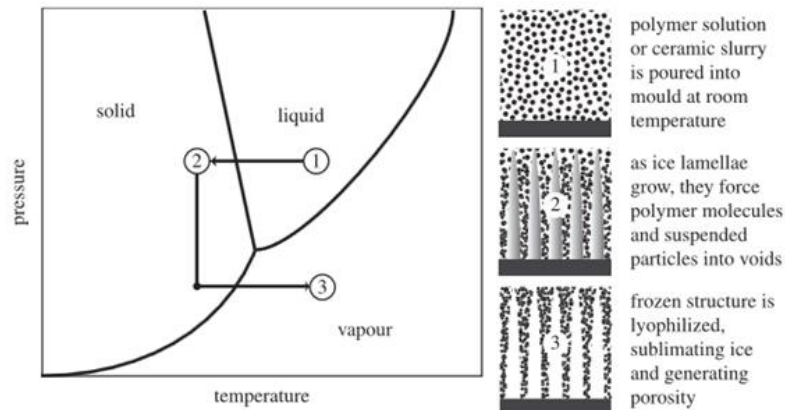


Figure 2. Phase diagram illustrating the phase changes of the liquid vehicle (water here) during the freeze-casting process (Wegst et al., 2010).

The critical point in the CPL operation is the maximum capillary force that must overcome all the pressure drops experienced by the fluid, as seen on Eq. (1). The condition under the CPL operates is that the total system pressure drop does not exceed the maximum capillary pumping pressure that the porous wick can provide. Due to the vapor penetration through the porous wick, the operating temperature of the system has a sudden increase when the capillary limit is exceeded. Thus, the capillary pumping system operation requires that the sum of the pressure drops in the components and in the transport lines must be smaller than the maximum capillary pressure head developed by the wick, i.e.,

$$\Delta p_{cap, max} \geq \Delta p_v + \Delta p_e + \Delta p_l + \Delta p_c \quad (1)$$

where, $\Delta p_{cap,max}$ is the maximum capillary pressure due to capillary force, Δp_v is the pressure drop due to vapor flowing through the vapor line, Δp_e is the pressure drop due the liquid flowing through the evaporator section, Δp_l is the pressure drop due to liquid flowing through liquid line and Δp_c is the pressure drop through the condenser head line.

The maximum capillary pressure, seen in Eq. (1), can be determined according to Young-Laplace equation, Eq. (2), where σ is the working fluid superficial tension, θ is the water contact angle and d_{eff} is the critical effective diameter of the porous element.

$$\Delta p_{cap,max} = \frac{4 \cdot \sigma \cdot \cos \theta}{d_{eff}} \quad (2)$$

In that way, the graduate porous sizes formed with the freeze casting method is exactly what the evaporator needs to provide a capillary pumping effect. For a typical fluid, Eq. (2) gives the maximum capillary pumping pressure related to the smaller pore sizes of the wick structure. In this work, the raw material used in the ceramic wick manufacturing is Alumina (Al_2O_3) powder Almatis CT3000 LS SG. According to the raw material supplier, the information about particle size and surface area are shown in Tab. 1.

Table 1. Powder information according to the raw material supplier.

Property	Typical
Specific surface area (BET)	7.80 m ² /g
Particle size/ D50	0.5 μ m
Particle size/ D90	2 μ m

Two different slurries were prepared changing the water/solid ratio: (i) samples A with 50 wt.% alumina and 50 wt.% water and (ii) samples B with 65 wt.% alumina and 35 wt.% water. The principal characteristics obtained were the porosity, capillary pressure, critical diameter and permeability.

The porosity was measured by weighting a set of samples with and without water intrusion and measuring the alumina powder density by picnometry (Multipicnometer QuantaChrome and Marte AL500C weighting scale) (Deschamps et al., 2015) and making use of Eq. (3),

$$\epsilon = (m_s - m_w) \left(\frac{m_s}{\rho_s} + \frac{m_w}{\rho_w} \right)^{-1} \times 100 \quad (3)$$

where m_s is the dry weight sample, m_w is the weight of the water impregnated sample, ρ_s is the measured density of alumina (3.85 g/cm³) and ρ_w is the water density (1,00 g/cm³).

The samples porous sizes and the capillary pressure is obtained through a capillary extrusion (Berti, 2008). The apparatus consists in two chambers divided by the ceramic wick sample that one wishes to characterize. In the chamber below there is nitrogen, whose pressure can be regulated by means of a needle valve. The gas pressure is measured by a pressure transducer (Omega PX309-030A5V). In the chamber above the porous element, there is a controlled amount of water. The upper chamber is transparent, so that it is possible to see when the nitrogen's pressure is high enough to push bubbles through the wick. The upper chamber is open, so that the pressure above the water column is always the atmospheric. The experiment begins opening the nitrogen needle valve gradually, in the lower chamber, and in this way increasing gradually the pressure below. The experiment ceased when bubbles start coming from the porous element to the upper chamber.

The capillary pressure and critical diameter are calculated considering Eq. (4) for the pressure drop due the porous size ($\Delta P_{l,w}$) and replacing with the Young-Laplace equation, to yield Eq. (5) and Eq. (6), respectively,

$$\Delta P_{cap} - \Delta P_{l,w} = 0 \quad (4)$$

$$\frac{4 \cdot \sigma \cdot \cos \theta}{d_c} - (p_g - \rho \cdot g \cdot h) = 0 \quad (5)$$

$$d_c = \frac{4 \cdot \sigma \cdot \cos \theta}{p_g - \rho \cdot g \cdot h} \quad (6)$$

where d_c is the critical pore diameter, σ is water surface tension (0.07197 N/m), θ is the water contact angle (here considered 0°), ρ is the water density (997 kg/m³), g is the gravitational acceleration (9.81 m/s²) and p_g is the gas pressure.

The permeability was determinate experimentally, using a similar apparatus as described for the capillary pressure. However, for the permeability one chamber is pressurized using water and the other side is now on atmosphere

pressure, and then the water mass flow rate is measured with a scale and a stopwatch. The pressure drop is also measured using this experiment.

Once the dimensions of the wick structure and the fluid properties of the system are known, and also the pressure drop (from permeability experiment) it is now possible to calculate the permeability from Darcy law, Eq. (7),

$$K = \frac{\mu_l \cdot Q \cdot L_w}{\Delta p_{l,w} \cdot A_w \cdot \rho_l} \quad (7)$$

where $\Delta p_{l,w}$ is the pressure drop, μ_l is the water viscosity ($8.9 \cdot 10^{-4}$ Pa.s), Q is the volumetric flow rate, L_w is the sample length, K is the sample permeability, A_w is the sample upper and bottom area and ρ_l is the water density (997 kg/m^3).

3. RESULTS AND DISCUSSION

For a better understanding of the structure that freeze casting method provides, the microstructure of the sintered body were observed using a scanning electron microscopy (SEM, HITACHI TM3030). Figure 3a shows a macro-morphology of sintered porous Al_2O_3 ceramic prepared from a suspension with 65 %wt. solid loading. No visible defects such as cracks or distortions were observed. Figures 3b and 3c present cross-sectional SEM micrographs of the sample, showing aligned straight pore features in a long-range order.

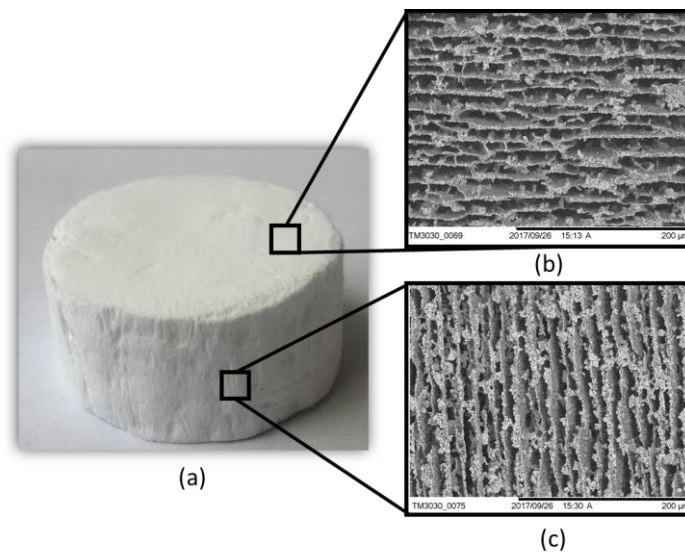


Figure 3. Macro and micro-morphologies of the porous Al_2O_3 ceramic prepared from 65 %wt. solid loading. (a) optical image; (b) SEM transverse cross-section; (c) SEM tangential cross-section.

Usually, the porous structure is a replica of original solvent structure. In this case, water was used as solvent, so that the porous ceramic exhibits lamellar porous structure due to the anisotropic interface kinetics of ice (Deville et al., 2007).

The microstructure can be modified by varying the concentration of the starting slurry. The final porosity of the material is directly related to the volume of water in the suspension. As can be seen in Tab. 2, samples A with 50 %wt. and samples B with 65 %wt. solid loading, the porosity increased with decreasing the solid loading.

Table 2. Porosity.

Sample	Average porosity (% vol.)
A	57.07
B	54.69

The corresponding capillary pressure for each group is presented Tab. 3 together with the calculated critical pore diameter.

It is important to remember that the freeze-casting method has, as its main characteristic, the variation of pore size, where in the lower region (where heat is quickly removed) there are the smallest pore diameters. Those smallest diameters correspond to the mean critical diameter presented in Tab. 3.

Table 3. Capillary pressure and critical diameter.

Sample	Average capillary pressure (kPa)	Average critical diameter (μm)
A	26.38 ± 0.41	10.91
B	13.19 ± 0.70	21.81

Table 4 show the permeability results for each group sample, predicted by Darcy law, Eq. (7).

Table 4. Permeability.

Sample	Permeability (m^2)
A	5.45×10^{-13}
B	1.95×10^{-13}

The found results are consistent, matching with other results found in the current technical literature (Berti, 2008; Berti et al., 2008; Choi et al., 2014; Deschamps et al., 2015; Semenic and Catton, 2009; Xu et al., 2013).

4. CONCLUSION

The wick structure obtained from the freeze casting method is able to meet the required characteristics of capillary evaporators, such as critical diameter and capillary pumping pressure, as it has been successfully tested in the lab. It is expected that new wick structures will operate satisfactorily when implemented in any evaporator of CPL, LHP or others two-phase heat transfer devices. In any case, the results are still preliminary. Further works are planned in order to get better results, better understanding and effective control of two-phase capillary pumping devices.

ACKNOWLEDGMENTS

This work is supported by CNPq as a financial support.

REFERENCES

- Berti, L. F. (2008). *Characterization of ceramic wicks for application in capillary pumping systems (in portuguese)*.
 Berti, L. F., Rambo, C. R., Reimbrecht, E. G., Bazzo, E., and Hotza, D. (2008). Production and characterization of ceramic porous elements for capillary evaporators (in portuguese). *Exacta*, 6(1), 57–64.
<https://doi.org/10.5585/exacta.v6i1.812>
 Berti, L. F., Santos, P. H. D., Bazzo, E., Janssen, R., Hotza, D., and Rambo, C. R. (2011). Evaluation of permeability of ceramic wick structures for two phase heat transfer devices. *Applied Thermal Engineering*, 31(6–7), 1076–1081.
<https://doi.org/10.1016/j.applthermaleng.2010.12.001>
 Chen, P. C., and Lin, W. K. (2001). The application of capillary pumped loop for cooling of electronic components. *Applied Thermal Engineering*, 21(17), 1739–1754. [https://doi.org/10.1016/S1359-4311\(01\)00045-X](https://doi.org/10.1016/S1359-4311(01)00045-X)
 Choi, J., Yuan, Y., Sano, W., and Borca-Tasciuc, D. A. (2014). Low temperature sintering of copper biporous wicks with improved maximum capillary pressure. *Materials Letters*, 132, 349–352.
<https://doi.org/10.1016/j.matlet.2014.06.090>
 Deschamps, I. S. (2016). *Investigation of Processing Parameters on Mechanical Strength for Porous Polymer Derived Ceramics by Freeze Casting*.
 Deschamps, I. S., Oro, M. V., Berti, L. F., Oliveira, M. de L., Fredel, M. C., and Bazzo, E. (2015). Processing and Morphological Analysis of a Two-Layer Ceramic Structure for Capillary Evaporators. In *23rd ABCM International Congress of Mechanical Engineering*. Rio de Janeiro: ABCM.
 Deville, S. (2008). Freeze-casting of porous ceramics: A review of current achievements and issues. *Advanced Engineering Materials*, 10(3), 155–169. <https://doi.org/10.1002/adem.200700270>
 Deville, S., Saiz, E., and Tomsia, A. P. (2007). Ice-templated porous alumina structures. *Acta Materialia*, 55(6), 1965–1974. <https://doi.org/10.1016/j.actamat.2006.11.003>
 Faghri, A. (1995). Capillary pumped loop systems. In *Heat pipe science and technology* (pp. 578–622).
 Reimbrecht, E. G., Fredel, M. C., Bazzo, E., and Pereira, F. M. (1999). Manufacturing and microstructural characterization of sintered nickel wicks for capillary pumps. *Materials Research*, 2(3), 225–229.
<https://doi.org/10.1590/S1516-14391999000300019>
 Reimbrecht, E. G., Nogoseke, M., Takahashi, A. R., Tabalipa, F., and Bazzo, E. (2001). Ceramic porous elements as an alternative for application in pumping systems (in portuguese). In *Ix Congresso Brasileiro De Engenharia E Ciências Térmicas* (Vol. 888, pp. 1–10).
 Semenic, T., and Catton, I. (2009). Experimental study of biporous wicks for high heat flux applications. *International Journal of Heat and Mass Transfer*, 52(21–22), 5113–5121.
<https://doi.org/10.1016/j.ijheatmasstransfer.2009.05.005>
 Wegst, U. G. K., Schecter, M., Donius, A. E., and Hunger, P. M. (2010). 1Biomaterials by freeze casting. *Philosophical*

Transactions. Series A, Mathematical, Physical, and Engineering Sciences, 368(1917), 2099–2121.

<https://doi.org/10.1098/rsta.2010.0014>

Xu, J., Zou, Y., Yang, D., and Fan, M. (2013). Development of biporous Ti₃AlC₂ ceramic wicks for loop heat pipe. *Materials Letters*, 91, 121–124. <https://doi.org/10.1016/j.matlet.2012.09.083>

Zhang, Y., Hu, L., Han, J., and Jiang, Z. (2010). Freeze casting of aqueous alumina slurries with glycerol for porous ceramics. *Ceramics International*, 36(2), 617–621. <https://doi.org/10.1016/j.ceramint.2009.09.036>

RESPONSIBILITY NOTICE

The authors are the only responsible for the printed material included in this paper.